Economic model-predictive control of building heating systems using Backbone energy system modelling framework

Topi Rasku*†, Toni Lastusilta*, Ala Hasan*†,
Rakesh Ramesh*, and Juha Kiviluoma*

September 20, 2023

Highlights

- Demonstrating the feasibility of building-level model-predictive control using Backbone for future system-wide demand-side management studies.
- Yearly cost savings around 3.1–17.5 % agree with existing literature, with the domestic hot water tank responsible of roughly three quarters of the savings.
- A typical 36-hour optimisation horizon seems sufficient to exploit most of the building-level flexibility.

Keywords: model-predictive control; building energy management; building energy flexibility; energy system modelling; energy system optimisation

Abstract

Accessing the demand-side management potential of the residential heating sector requires sophisticated control capable of predicting buildings' response to changes in heating and cooling power, e.g. model-predictive control. However, while studies exploring its impacts both for individual buildings as well as energy markets exist, building-level control in large-scale energy system models has not been properly examined. In this work, we demonstrate the feasibility of the open-source energy system modelling framework Backbone for simplified model-predictive control of buildings. Hourly rolling horizon optimisations were performed to minimise the costs of flexible heating and cooling electricity consumption for a modern Finnish detached house and an apartment block with ground-to-water heat pump systems for the years 2015–2022. Compared to a baseline using a constant electricity price signal, optimisation with hourly spot electricity market prices resulted in 3.1–17.5 % yearly cost savings depending on the simulated year, agreeing with comparable literature. Furthermore, the length of the optimisation horizon was not found to have a significant impact on the results beyond 36 hours. Overall, the simplified model predictive control was observed to behave in a reasonable manner, lending credence to the integration of simplified building models within large-scale energy system modelling frameworks.

*VTT Technical Research Centre of Finland Ltd., P.O.Box 1000, FI-02044 VTT, Espoo, Finland

†Corresponding authors: topi.rasku@vtt.fi, ala.hasan@vtt.fi

1 Introduction

Electrification of traditionally fossil-fuelled sectors like transportation and heating is one of our more promising decarbonisation pathways [1]. Unfortunately, most of our renewable electricity generation potential originates from variable sources, leaving power utilities scrambling for flexibility capable of mitigating said variability [2]. This newfound demand for flexibility has rekindled interest in various demand-side management (DSM) measures as a potential alternative for investing in additional energy storage or dispatchable generation capacity [3].

Buildings are the largest consumers of energy worldwide, responsible for over 30 % of the global final energy consumption [4] and expected to increase by around 30 % in another twenty years [5]. Furthermore, heating, ventilation, and air conditioning (HVAC) systems maintaining comfortable indoor temperature conditions can account for more than 30–60 % of a buildings total energy consumption [6, 7, 8]. Thus, the heating and cooling sector holds significant DSM potential [9], but accessing it requires sophisticated control of the buildings' systems. While rule-based control can be effective in reducing energy consumption in buildings [10, 11, 12], it is incapable of properly accounting for the buildings future thermal response. Model-predictive control (MPC) overcomes this issue, making it more suitable for harnessing the flexibility in buildings [13].

On the level of individual buildings, MPC is typically employed for optimal control of the buildings' systems, often utilising detailed technical parameters or plentiful real-time measurements [14, 15]. However, studying the impacts of such controls on energy-market scale makes holistically modelling each building infeasible and requires the use of dedicated energy system models. Furthermore, obtaining sufficient input data for detailed building models becomes increasingly more difficult as the scale or the modelled energy system increases, encouraging more simplified and robust modelling approaches. While there are studies examining the energy-system impacts of different power-to-heat measures [9], the integration of building-level and large scale energy system models is still not well understood.

The remainder of this paper is organised as follows: Section 1.1 summarises the relevant scientific background, while Section 1.2 highlights the contribution of this paper. The modelled buildings are detailed in Section 2.1, and the MPC implementation using the Backbone energy system modelling framework is explained in Section 2.2. Finally, the optimisation results are presented in Section 3, their implications explored in Section 4, with conclusions drawn in Section 5.

1.1 Background

While some features of MPC can be traced back as far as the 1950s, it did not see industrial applications until the mid-1970s with access to cheaper and more reliable computer-based control [16]. In modern-day society with near-ubiquitous computers, MPC has become appealing for smaller-scale applications as well, such as building HVAC control [14]. Furthermore, MPC has been successfully employed for building HVAC systems to reduce energy demand and costs, as well as increase the self-consumption of on-site renewables, all while satisfying the occupants comfort [17, 18]. The existing literature on building-level MPC is vast, as evidenced by the recent reviews by Drgoňa et al. [14], Yao and Shektar [17], and Taheri et al. [18]. Examples of economic MPC studies including a small residential building with a heat pump system with floor heating depicted using a third-order resistance-capacitance (RC) model [19], a multi-zone commercial building with variable air volume cooling systems modelled using EnergyPlus with controls optimised using MATLAB [20], real-world multi-objective MPC trials for commercial buildings in Australia [21], a single-family house with multiple local renewable energy systems [22], as well as a small energy community of four single-family houses [23]. City-scale economic scheduling studies have also been performed e.g. for Copenhagen [24] and Helsinki [25], although focusing more on the district heating system than the buildings themselves. Recent advances in machine learning have also increased interest in data-driven predictive control for building applications [15].

All of the above-mentioned studies model build-

ings or cities strictly as "price-takers", meaning that any change in their energy consumption is assumed not to affect the operation of the overarching energy system and the balance of the spot energy markets. While this is true for current day-ahead spot electricity markets, if DSM by flexible buildings becomes mainstream and significant numbers of buildings begin shifting their consumption in unison, markets will be forced to account for the reacting demand in some manner. Thus, there have been several studies examining the impacts widespread of building-level flexibility on the energy-market-scale as well [9]. Most noteworthy among them are perhaps the studies by Hedegaard et al. [26, 27], pioneering the integration of simplified building RC models with the large-scale energy system model Balmorel for studying investments into flexible residential heat pump systems for wind power integration. Similar approaches have since been applied for studying peak-net demand increase caused by electrification of heating via heat pumps in the UK [28], impact of market penetration of electric heating demand response in Belgium [29] and Finland [30], comparing different flexible heating technologies in Germany [31], as well as impacts of pan-European multi-flexibility-source load-shifting [32].

1.2 Contribution

Despite the wealth of studies on the subject of building-level MPC and its implications for energy system operations discussed in the previous section, to the authors' best knowledge, there has never been an attempt to examine whether the building models employed within large-scale energy system modelling frameworks can perform reasonable building-level MPC. While the results of the previous energy-system-scale studies have not indicated reasons to doubt the used approach, performing building-level simulations helps further validate it, as well as better understand its limitations. Thus, this paper aims to address this research gap by demonstrating that Backbone can capture the key dynamics of such control, and briefly investigates the impact of different rolling horizon optimisation parameters on the results. This is a missing stepping-stone toward system-level studies, where large-scale scenario analysis is supplemented by more detailed local-level modelling, helping improve the reliability of the results and possibly correct large scale models through iterative approaches. Furthermore, the investment optimisation capabilities present in many large-scale energy system optimisation frameworks facilitate comparing the economic viability of widespread building-level DSM solutions against competing flexibility options on national scales.

2 Materials and methods

A significant share of existing large-scale energy system modelling frameworks is based on mixed-integer linear programming (MILP), as concurrent solvers can efficiently handle very large problems [33]. This severely limits applicable building modelling options, however, as most detailed physics-based white-box models cannot be integrated directly due to their reliance on non-linear functions [34]. Similarly, data-driven black-box models typically employ mathematical frameworks that cannot be implemented in a MILP-compatible manner [15]. Fortunately, simplified grey-box RC-modelling approaches have been shown to sufficiently capture the temperature dynamics in buildings, and can be integrated directly into MILP problems [35]. Although, while RC models are ideal for large-scale energy system model integration, detailed white-box models or data-driven black-box models typically perform better in terms of accuracy, reliability, and adaptability when it comes to building-level MPC applications with access to detailed technical properties and measurement data from the building [14, 15].

The remainder of this section is organised as follows: Section 2.1 first presents the modelled buildings as well as a brief overview of the simplified RC model, before Section 2.2 introducing the key aspects of Backbone used for the MPC. Furthermore, the raw data and the code for processing the data for the case study have been made available through Zenodo for interested readers [36].

2.1 Modelled buildings

Residential buildings make up most of existing building stocks, and as such, are of key interest for building MPC. In terms of the flexibility in space heating demand, the effective thermal mass of the building is a potentially important factor. Thus, this work included both a light wooden-framed detached house (DH) and a heavy concrete apartment block (AB), illustrated in Figure 1 and described in more detail in Tables 1 and 2 respectively. The modelled buildings were based on the readily-made example buildings from the IDA ESBO v1.13 [37], adhering to the 2012 Finnish regulations [38]. However, ventilation heat recovery units were disabled for simplicity, as well as to keep the building models identical to the previous IDA ESBO validations [39].

The IDA ESBO building models were reduced into simplified RC models with only three temperature nodes depicting each building, namely the indoor air and furniture node, and the heavy and light structural mass nodes, illustrated in Figure 2. This nodal configuration had the most robust performance in terms of uncertainties related to the structural and solar gain properties in previous IDA ESBO validations [39], and the same RC models were reused in this work with the addition of a domestic hot water (DHW) tank temperature node to represent its storage capacity. A summary of the key indicators used for validating the RC models against IDA ESBO is presented in Table 3. For the sake of brevity, the RC model validation is not reproduced here, and interested readers are instead kindly referred to the aforementioned previous work [39]. While more accurate RC models could undoubtedly be obtained via state-of-the-art calibration routines [40] and processed for Backbone, these robust models were chosen for this demonstration as they better represent the intended use case on the energy-system scale, where detailed measurement or simulation data for proper calibration is often lacking. The indoor air and DHW tank node temperatures were constrained between 21–25°C and 60–90°C respectively based on the Finnish building code [41, 42], governing the available flexibility in space and water heating demands.

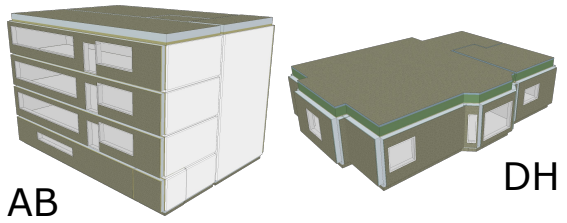

Figure 1: Illustrations of the modelled apartment block (AB) and detached house (DH). Note that the shown IDA ESBO model for AB represents only one half of the entire building, and is mirrored over the partition walls shown in light grey to form the full building.

Time-varying prices make the use of economic MPC more worthwhile, so the buildings were modelled with ground-to-water heat pump (G2WHP) systems for both space and water heating. For simplicity, the G2WHP was modelled using a simple seasonal performance factor (SPF) of 2.5, as suggested by Finnish building code calculation guides for G2WHPs with 60°C hydronic radiator heat distribution systems typical in Finland [43]. Similarly, the buildings were equipped with ground-source cooling systems with SPF of 30 [43] to ensure feasible indoor air temperatures during summer. While temperature-dependent coefficients of performance for the heat pumps could be used to improve the accuracy of the modelling, they were purposefully avoided in order to permit calculating a more realistic baseline using Backbone, as explained in Section 3.1. The heating and cooling systems were assumed to be sized such that they could handle all heating and cooling demand in the modelled buildings without the need of auxiliary systems.

The G2WHP was also used for pre-heating DHW up to 60°C, but topping up to the maximum 90°C permitted for the modelled DHW tanks using resistance heaters reduced the overall SPF to ≈ 1.58. The DHW storage tanks were sized to store roughly two thirds of the assumed daily DHW demand with the permitted temperature range, resulting in 250 and 3000 litre tanks for the modelled detached house and apartment block respectively. The sizing, heat losses and other relevant technical properties of the DHW

Table 1: Key properties of the modelled detached house (DH).

Gross floor area	135.56 m^2
Number of storeys	1
Room height	2.6 m
Ventilation air change rate	0.55 times per hour
Infiltration air change rate	0.06 times per hour

Structure	**Description**	**U [W/m^2K]**	**C_{eff} [kJ/m^2K]**
Roof	13 mm plasterboard finish, 482 mm mineral wool insulation, asphalt roll roofing.	0.09	21.96
Exterior wall	13 mm plasterboard finish, 237 mm mineral wool insulation, 20 mm board exterior.	0.17	15.61
Base floor	20 mm autoclaved aerated concrete finish, 200 mm concrete slab, 207 mm expanded polystyrene insulation.	0.18	487.49
Partition wall	Timber frame, 13 mm plasterboard finish on both sides.	—	18.28

Table 2: Key properties of the modelled apartment block (AB).

Gross floor area	1608.19 m^2
Number of storeys	4 *(counting the basement)*
Room height	2.7 m
Ventilation air change rate	0.67 times per hour
Infiltration air change rate	0.04 times per hour

Structure	**Description**	**U [W/m^2K]**	**C_{eff} [kJ/m^2K]**
Roof	10 mm mortar finish, 150 mm concrete slab, 486 mm mineral wool insulation, asphalt roll roofing.	0.09	412.71
Exterior wall	10 mm mortar finish, two 100 mm concrete slabs sandwiching 252 mm mineral wool insulation.	0.17	263.25
Base floor	20 mm autoclaved aerated concrete finish, 200 mm concrete slab, 207 mm expanded polystyrene insulation.	0.18	487.49
Partition wall	160 mm concrete slab.	—	375.28
Separating floor	20 mm autoclaved aerated concrete finish, 150 mm concrete slab.	—	334.34

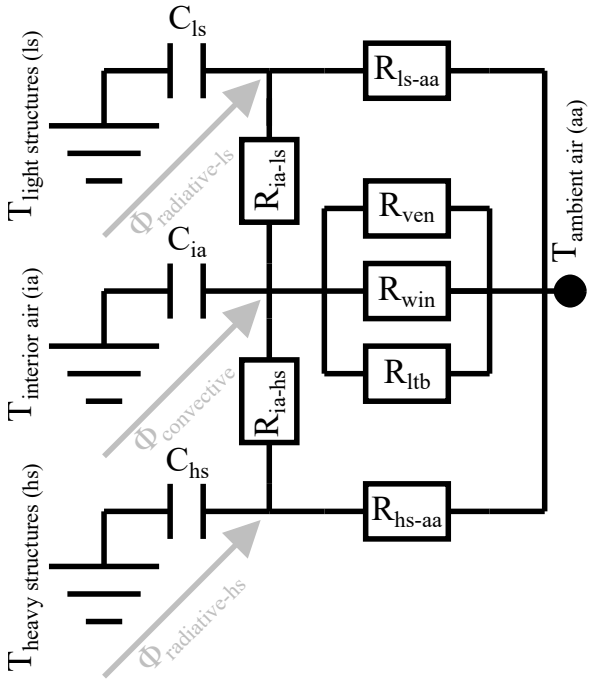

Figure 2: The resistance-capacitance model for the buildings. C denotes effective thermal masses of the model nodes, R represents the thermal resistances between the nodes, and Φ indicates the impact of solar and internal heat gains, as well as radiative sky losses. The interior air (ia) is directly in contact with ambient air (aa) via ventilation (ven), the windows (win), and the linear thermal bridges (ltb) through the envelope structures.

Table 3: Summary of the key indicators for the full-year free gross-floor-area-averaged indoor air temperature comparisons with IDA ESBO performed in [39] for the used RC models.

Indicator	**DH**	**AB**
Root-mean-sqare error [°C]	0.286	0.378
Maximum error [°C]	1.23	1.48
Mininum error [°C]	−0.937	−0.671

tanks were based on typical values presented in the Finnish building code calculation guides [42]. It is worth noting that the heat losses from the DHW tanks were assumed to be fully utilisable, contributing to the heat gains on the interior air as shown in Figure 4. While this is not often the case in reality, it simplifies the model and is sufficient for the purpose of this paper.

The internal heat gains and DHW demand profiles were based on simple typical daily profiles in the national calculation guides [42] presented in Figure 3. The internal heat gains include the assumed effect of inhabitants, appliances, and lighting, but were aggregated into a single total heat gain profile for simplicity. Using identical profiles for both the modelled detached house (DH) and apartment block (AB) is not ideal, as the profiles are dependent on the building type in reality. However, the identical profiles are acceptable for the purpose of this paper. Meanwhile, the ambient temperatures, solar heat gains, and radiative sky losses were processed using ArchetypeBuildingModel.jl [44] and PyPSA/atlite [45] based on weather data from the ERA5 global reanalysis dataset [46] for the coordinates of the Helsinki-Vantaa airport.

2.2 Backbone MPC implementation

Backbone is an open-source MILP-based large-scale energy system modelling framework written in GAMS, primarily developed for solving expansion planning [47], hydro-thermal scheduling [48], and unit commitment [49] problems. In order to accommodate such a broad scope of problems, the temporal, stochastic, and system depictions were designed in a generic and adaptable manner, allowing users to define radically different problems via input data and definitions. Here, only the key aspects of Backbone relevant for building-level MPC are presented, and readers interested in further details are kindly referred to the paper by Helistö et al. [50] containing the full model formulation.

At its core, Backbone is cost minimisation model, where the objective function depicts the total system costs of generating all the energy required to satisfy the demand in the modelled system, as well

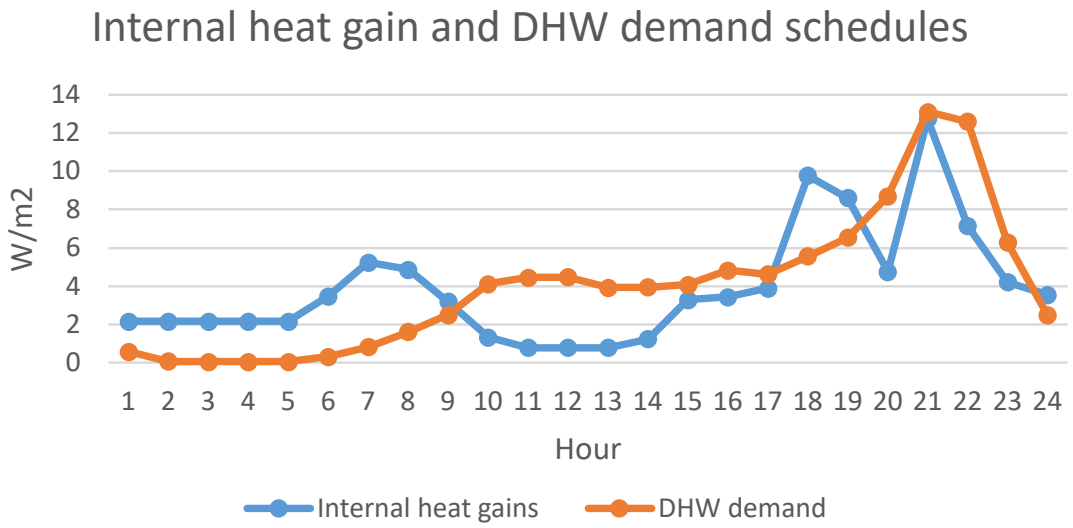

Figure 3: Assumed daily schedules of internal heat gains and as domestic hot water demand [42].

as installing new or replacing old assets. As such, Backbone is primarily suited for economic MPC of buildings, although other objectives could also be accommodated either by pricing them in the objective function, or by introducing custom constraints to the problem. In this work, Backbone was configured to perform rolling horizon economic optimisation depicting MPC, and it is important to understand the following distinctions going forward:

Time step t refers to the time indices of the model, and Δ_t refers to the length of time step t in hours. In this work, only hourly time resolution was used $\Delta_t = 1\,\mathrm{h}\;\forall t$.

Optimisation interval refers to the frequency of the rolling horizon optimisation. E.g. a 6-hour interval meant that results were saved for the first six hours of each solve, before moving forward by six hours for the next solve.

Optimisation horizon $\mathbb{T}$ refers to the set of time steps t in each solve. E.g. with a 36-hour horizon, optimal control was always solved for the next 36-hours before rolling.

The key costs for building-scale MPC typically only include the costs of imported energy, reducing the simplified MPC optimisation problem to the following:

$$\min_{\boldsymbol{v}} \quad f = \sum_{t\in\mathbb{T}}\sum_{u\in\mathbb{U}}\left[\tau^{\text{ts\_price}}_{import,t} v^{\text{gen}}_{import,u,t}\Delta_t\right] \tag{1}$$

$$\text{s.t.} \quad \frac{p^{\text{energyCapacity}}_n}{\Delta_t}\left(v^{\text{state}}_{n,t} - v^{\text{state}}_{n,t-\Delta_t}\right) = -p^{\text{selfDischargeLoss}}_n v^{\text{state}}_{n,t} - \sum_{n'\in\mathbb{N}_n}\left[p^{\text{diffCoeff}}_{n,n'}(v^{\text{state}}_{n,t} - v^{\text{state}}_{n',t})\right] + \sum_{u\in\mathbb{U}_n}\left[v^{\text{gen}}_{n,u,t}\right] + \tau^{\text{influx}}_{n,t} \quad \forall n\in\mathbb{N}, t\in\mathbb{T} \tag{2}$$

$$v^{\text{gen}}_{import,u,t} = p^{\text{slope}}_u v^{\text{gen}}_{n,u,t} \quad \forall u\in\mathbb{U}, n\in\mathbb{N}_u, t\in\mathbb{T}, \tag{3}$$

$$\text{and} \quad p^{\text{lowerLimit}}_n \le v^{\text{state}}_{n,t} \le p^{\text{upperLimit}}_n \quad \forall n\in\mathbb{N}, t\in\mathbb{T}, \tag{4}$$

$$0 \le v^{\text{gen}}_{import,u,t} \le p^{\text{capacity}}_{import,u} \quad \forall u\in\mathbb{U}, n\in\mathbb{N}_u, t\in\mathbb{T}, \tag{5}$$

where p, v, and τ denote different parameters, variables, and time series respectively, with their names indicated by the superscript and indices by the sub-

script. By exploiting Backbones generic design, its energy networks can be parameterised to represent building RC models as illustrated in Figure 4. The set $\mathbb{U}$ contains all heating and cooling equipment units u and the set $\mathbb{N}$ contains all the temperature nodes shown in the figure. The objective function in Eq. (1) is relatively straightforward, representing the total cost of imported electricity for all units $u \in \mathbb{U}$ and over the entire optimisation horizon $t \in \mathbb{T}$, where *ts_price* is the electricity price time series in €/Wh, and the *gen* variable represents the electricity consumed in W by the heating and cooling units. Please note that Eqs. (1)–(5) have been considerably simplified from the full Backbone formulation [50], omitting unused features like controlled energy transfer and spill variables, variable and fixed costs related to units and energy transfer, capacity expansion related investment costs and discount factors, as well as forecast and scenario indices and their weights.

When implementing simple building RC models within Backbone via the energy balance constraint in Eq. (2), the *state* variables represent the temperature of the building nodes in K, the *energyCapacity* parameter depicts the heat capacity of said nodes in Wh/K, while the *diffCoeff* determines the heat transfer coefficients between them in W/K. The heating equipment are depicted simply using the *gen [W]* variables, either adding energy when heating, or removing energy when cooling. Here, the subsets $\mathbb{N}_n$ and $\mathbb{U}_n$ are used to indicate which nodes n' and units u are connected to the energy balance on the current node n, as illustrated by Figure 4. Unfortunately, Backbone does not have dedicated parameters for supporting building-specific interactions like heat losses into the ambient air, solar gains, or internal heat gains in Eq. (2), requiring them to be pre-processed to fit into Backbone data structure. The ambient temperature interaction can be separated into its indoor-air and ambient-air-temperature-dependent constituents, and implemented via a combination of the *selfDischargeLoss [W/K]* parameter and the *influx [W]* time series. Similarly, since solar and internal heat gains are assumed independent of the variables, their effects can be added to the *influx* time series as well. For readers interested in further details on the building RC model processing for Backbone, please refer to the ArchetypeBuildingModel.jl online documentation [44].

The energy conversion constraint in Eq. (3) governs the operation of the heating and cooling units $u \in \mathbb{U}$, namely the G2WHP and ground-source cooling, by enforcing a fixed ratio between the input and output energy of each unit. In Backbone, the *slope* parameter represents the heat rate of unit u, which is the inverse of its efficiency, or the SPF in our case. Here, it is worth noting that space heating and water heating using the G2WHP are treated as independent units as shown in Figure 4 for simplicity. Furthermore, since the ground-source cooling system unit is removing heat from the indoor air node, its *slope* parameter and thus also its *gen* variable are negative.

Eq. (4) sets the bounds for the *state* variables between the given *lowerLimit [K]* and *upperLimit [K]* parameter values. While all of the temperature nodes presented in Figure 4 were constrained for computational reasons, the limits for the light and heavy structure nodes were set loose enough not to impact the operation of the MPC, leaving the interior air and DHW tank temperature limits discussed in Section 2.1 to govern the flexibility available to the MPC. Similarly, Eq. (5) sets the upper bounds for the electricity import *gen* variables via the *capacity [W]* parameters based on the assumed system sizing discussed in Section 2.1.

For the simulations presented in Section 3, Backbone was configured to perform 8736-hour rolling horizon optimisations depicting the MPC of the modelled buildings. Essentially, the MPC optimisation problem presented in Eqs. (1)–(5) was solved for the desired optimisation horizon $\mathbb{T}$, the resulting optimal values for the *state* and *gen* variables were fixed for the chosen optimisation interval, and the problem was rolled forward by the interval to be resolved for the next horizon. In order for the rolling horizon optimisation to obtain results for the last hours of the simulation, the horizon can extend beyond the current year. Backbone deals with this by recycling data from the beginning of the year to make up for the missing information, which can result in unrealistic swings in electricity prices and ambient conditions. Thus, the length of the simulations was limited to

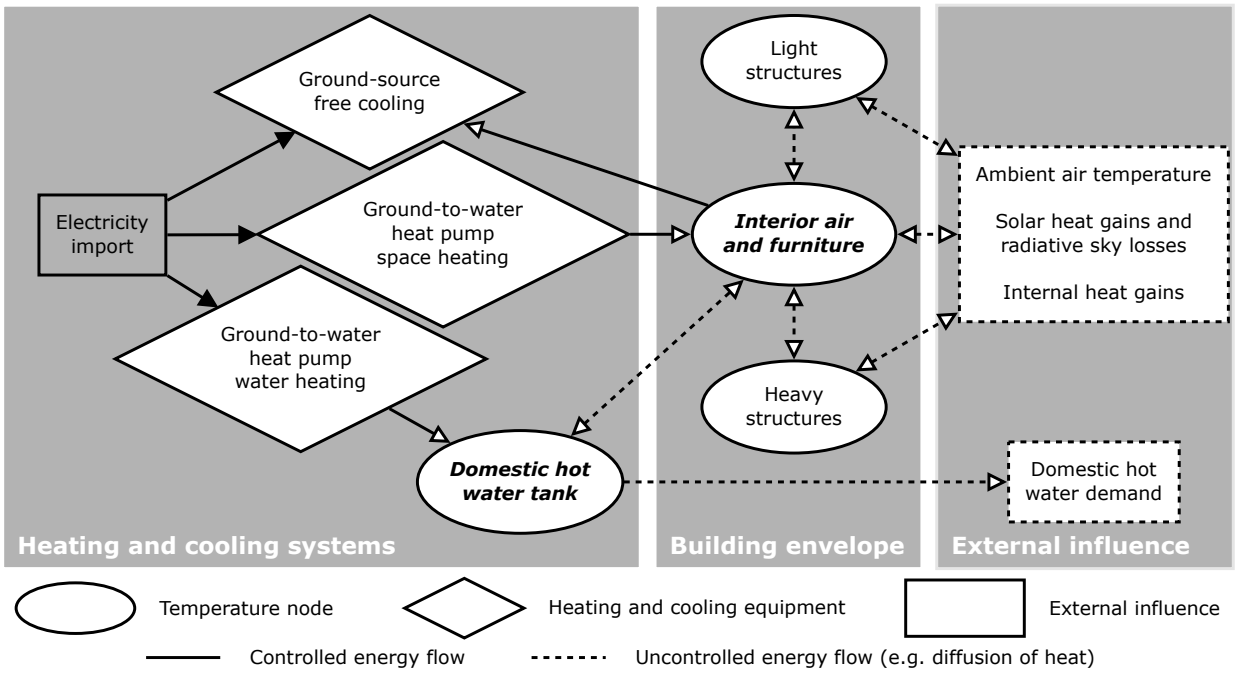

Figure 4: Energy system structure for the modelled buildings.

8736 hours to avoid "overshooting" the year when using a 168-hour optimisation interval, as well as to mitigate any potential impacts of the end of the year on the results.

3 Results

In order to demonstrate that the Backbone energy system modelling framework can capture the essence of simplified building-level MPC, simulations were performed both using constant and time-varying hourly spot electricity prices for the years 2015–2022 as the control signal. The simulations using the constant electricity prices served as a baseline to compare the spot price simulations against, allowing us to ensure the MPC behaved logically with the given objective. The main results are presented in Section 3.1, while Section 3.2 presents further results with longer optimisation intervals and horizons in order to analyse their impact on the main results.

Electricity spot market prices were obtained from ENTSO-E [51], but in order to arrive at more realistic consumer prices, electricity taxes of 22.53 €/MWh for Finnish residential consumers [52] and an assumed profit margin of 2.40 €/MWh were included. For the baseline simulations, yearly average prices were used as the control signal in the objective function, but the final cost values were calculated using the resulting hourly electricity consumption and the hourly spot market prices in order to keep the costs comparable.

Perfect information about future electricity prices and weather conditions were assumed, regardless of the used optimisation horizon. While Backbone could solve rolling horizon optimisation with a single forecast or even stochastic forecasts, these were omitted for simplicity and to keep the focus on model performance. All of the simulations were performed on a laptop with a *11th Gen Intel(R) Core(TM) i7-1185G7 @ 3.00GHz (4 cores)* processor and 32 GB of RAM, using Cbc [53] to solve the rolling horizon optimisation problems generated by Backbone.

3.1 MPC cost savings

The main MPC simulations employed 12-hour rolling horizon optimisation solved every hour, representing a horizon for which the prices are always known in current day-ahead markets. Figure 5 presents an overview of the MPC behaviour for the year 2022 when provided with both constant and hourly spot electricity prices as the control signal. As seen in Figure 5a, the MPC had no incentive to utilise the available flexibility given constant electricity prices, thus expending the least amount of effort to maintain permitted node temperatures. Essentially, the MPC behaved as intended, enabling its use as the baseline for the spot electricity price simulations. However, it is worth noting that the baseline can be calculated in this manner only thanks to the simplifying assumption of a fixed SPF for the G2WHP systems. Otherwise, Backbone would exploit the flexibility in heating and cooling demand to shift heat pump consumption towards hours with better coefficients of performance, making the baseline unreasonable for the intended comparisons. Meanwhile, Figure 5b using spot electricity prices shows the MPC taking advantage of the available flexibility, as the DHW tank and interior air node temperatures can be seen to vary throughout the year. The full-year results are only presented for the detached house, as there is little visible difference in the overall behaviour of the apartment block.

Figure 6 presents a more detailed view of the MPC operation of the spot electricity price simulations during one week in February 2022. The DHW tank can be seen charging mostly during the cheaper hours of the night, with some extra heating during comparatively cheap hours during the day as well. Since both buildings had the same typical DHW demand profile, the DHW tanks were utilised in near-identical manner, which can also be observed for the full year duration curve presented in Figure 7b. On the other hand, the space heating system can be seen overheating the interior air only before sharp increases in electricity prices. Curiously, comparing the space heating system operation for DH and AB in Figure 6, the DH can be seen to utilise its flexibility slightly more often. Figure 7a similarly shows a larger difference between the interior air node temperature of the DH compared to the AB throughout the year, corroborating the previous observation. Interestingly, the AB also utilised its space cooling flexibility enough to reduce the number of high-temperature hours inside the building.

Table 4 presents a summary of the key results from the simulations, focusing on comparing the performance of the spot electricity price optimised MPC against the baseline. The total yearly heating and cooling costs ranged between 417–1477 € for the DH and between 4049–14252 € for the AB depending on the modelled year, with yearly savings ranging between 17–269 € *(3.1–15.4 %)* and 196–3020 € *(3.6–17.5 %)* for the DH and AB respectively. However, the yearly energy consumption compared to the baseline was slightly increased by around 1.1–3.0 % for the DH and around 1.3–2.8 % for the AB due to the additional heat losses caused by utilising the heat storage capacity in the building. The DHW tank was found to be responsible for the majority of the cost savings, ranging from 70.4–83.4 % and 74.1–88.0 % of the savings for the DH and AB respectively depending on the simulated year.

The yearly fluctuations in the DHW share of savings were at least partially due to the yearly variations in space heating demand presented in Tables 5 and 6, driven by the heating degree days (HDD), as shown in Figure 8. During colder years with more HDDs, the space heating demand increases, which in turn seemed to allow more flexibility from the space heating system. Meanwhile, the flexibility available from the DHW demand was essentially identical between the years, resulting in the DHW share of savings fluctuating between the years. Fluctuating electricity prices also play a part in determining the DHW share of savings, but due to the complex dependencies between electricity prices, weather conditions, and the properties of space and water heating flexibility, their impacts are extremely difficult to analyse.

3.2 Impact of forecast horizon

Since the results in Section 3.1 used a rather conservative forecast horizon length of 12 hours, impacts

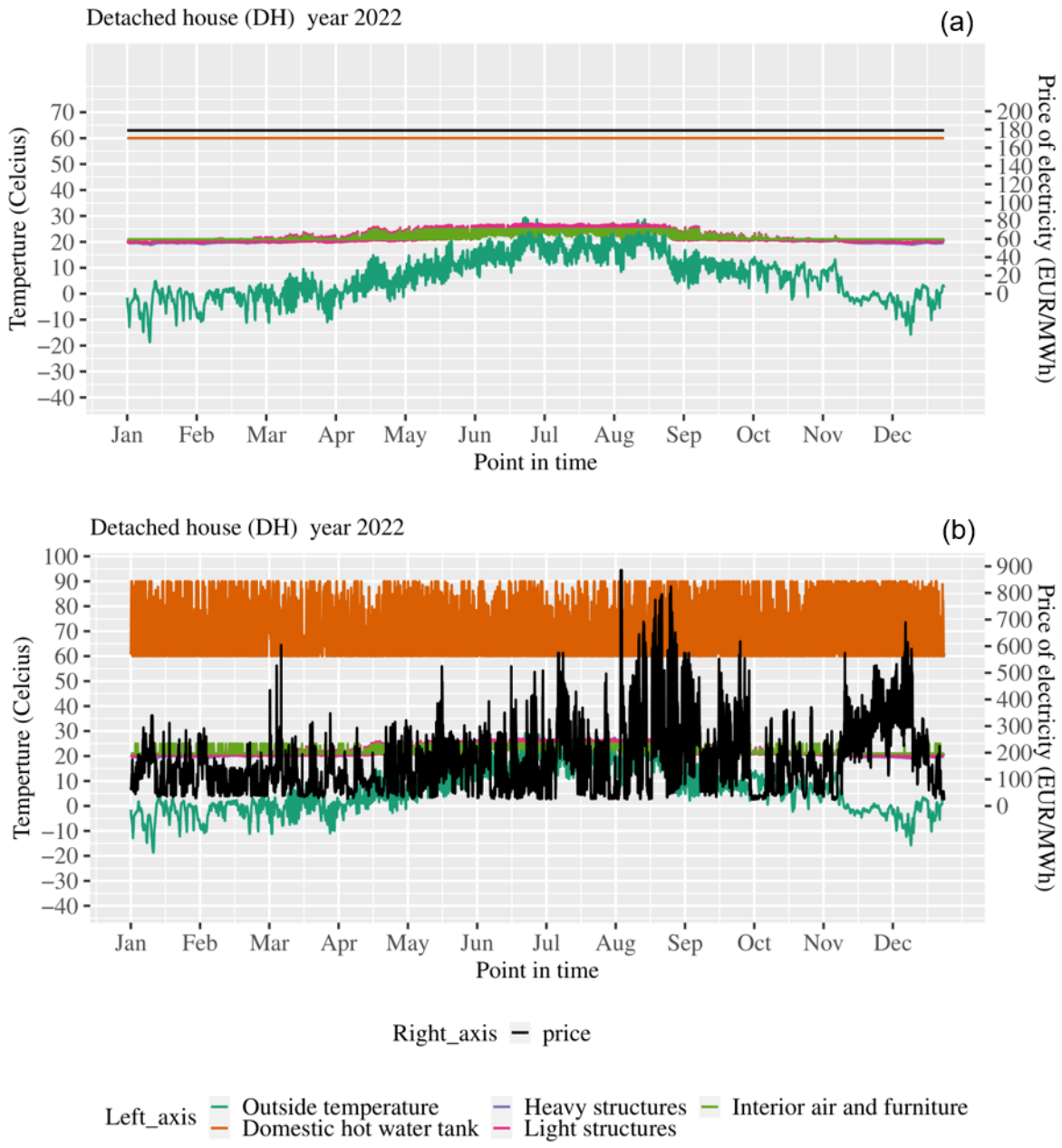

Figure 5: Full year detached house simulation results using constant (a) and spot (b) electricity price control signals for the year 2022.

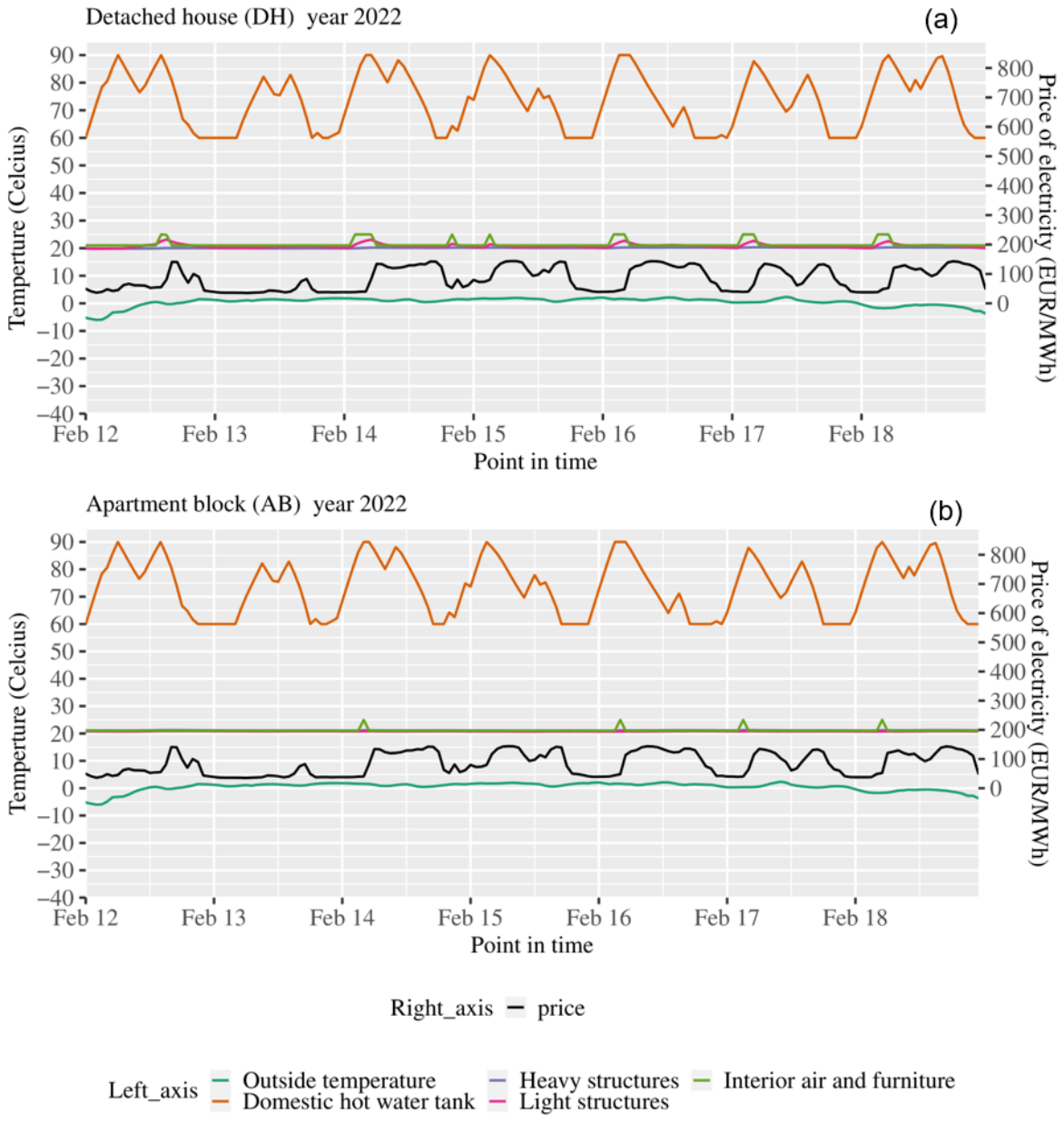

Figure 6: Example spot price optimisation results for week 7 in 2022 for the DH (a) and AB (b) respectively.

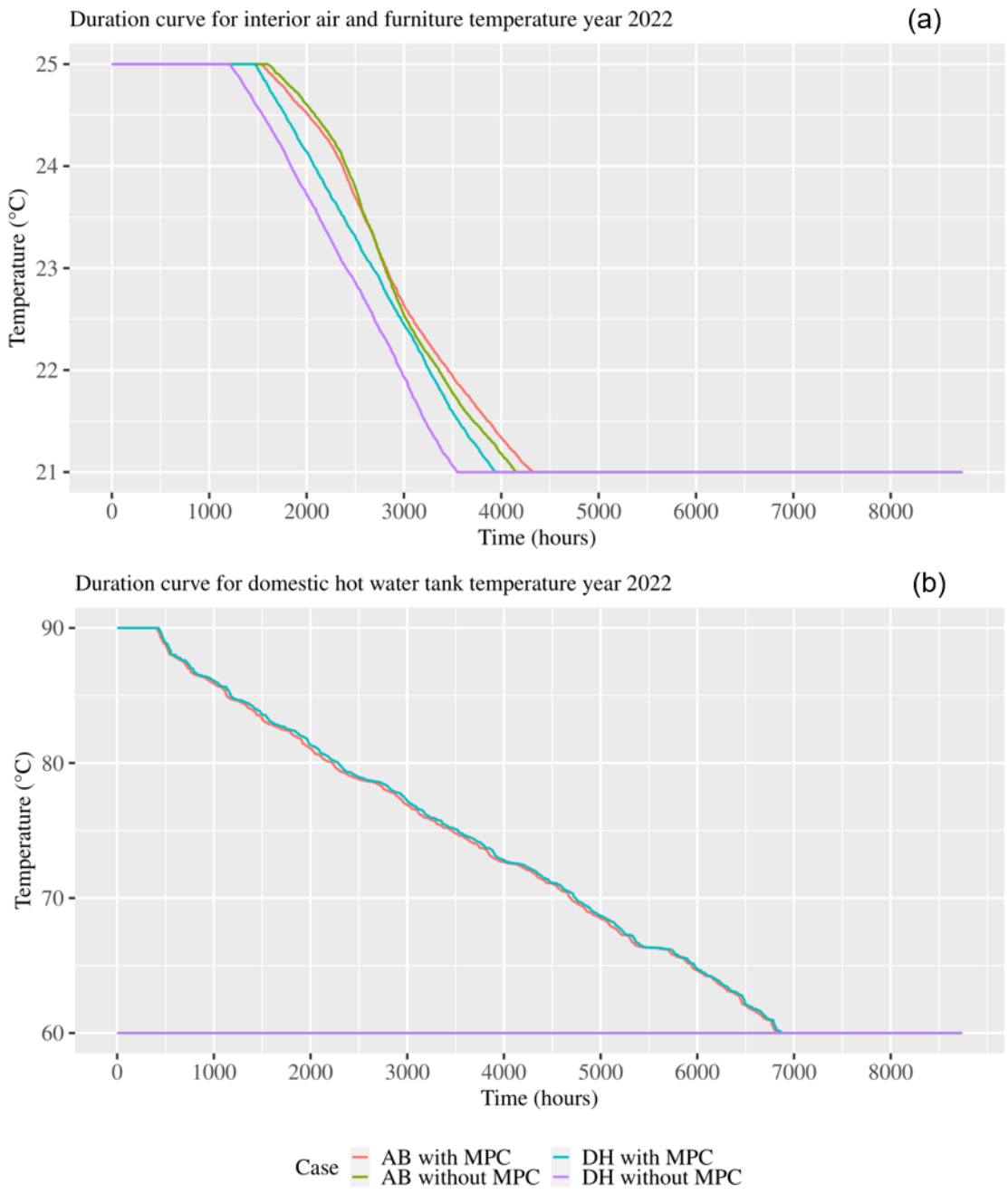

Figure 7: Duration curves for interior air and furniture temperature (a) and domestic hot water tank temperature (b) in 2022. Note that in (b), the *AB without MPC* overlaps with the *DH without MPC*, as neither had any incentive to charge the DHW tank temperature in the constant price baseline.

Table 4: Key yearly results for 2015–2022, hourly optimisation interval and 12-hour horizon.

Detached house (DH)	**2015**	**2016**	**2017**	**2018**	**2019**	**2020**	**2021**	**2022**
Baseline consumption [kWh]	8775	9782	9451	9732	9353	8518	9988	9418
MPC consumption [kWh]	8901	9902	9552	9836	9478	8691	10188	9699
— Increase [kWh]	126	120	101	104	125	173	200	280
— Relative increase [%]	1.4	1.2	1.1	1.1	1.3	2.0	2.0	3.0
Baseline cost [€]	494	581	553	700	666	464	1106	1746
MPC cost [€]	462	557	536	678	638	417	997	1477
— Savings [€]	32	24	17	22	28	47	109	269
— Relative savings [%]	6.6	4.0	3.1	3.2	4.1	10.1	9.9	15.4
— DHW share of saving [%]	83.4	75.4	71.6	70.4	76.6	81.6	75.9	83.4
Apartment block (AB)								
Baseline consumption [kWh]	84814	94639	90863	94270	90174	82618	95968	90281
MPC consumption [kWh]	86332	96055	92101	95459	91655	84478	97919	92772
— Increase [kWh]	1517	1416	1238	1189	1481	1859	1951	2491
— Relative increase [%]	1.8	1.5	1.4	1.3	1.6	2.3	2.0	2.8
Baseline cost [€]	4804	5648	5349	6827	6454	4568	10709	17272
MPC cost [€]	4433	5381	5153	6578	6137	4049	9462	14252
— Savings [€]	371	267	196	249	317	519	1247	3020
— Relative savings [%]	7.7	4.7	3.7	3.6	4.9	11.4	11.6	17.5
— DHW share of savings [%]	86	78.7	74.8	74.1	78.8	87.5	78.5	88.0

Table 5: Detailed yearly results per m^2 for the detached house (DH).

Consumption [kWh/m²]		**2015**	**2016**	**2017**	**2018**	**2019**	**2020**	**2021**	**2022**
Heating	Baseline	32.05	39.41	37.06	38.85	36.18	30.07	40.75	36.62
	MPC	31.43	38.78	36.46	38.31	35.54	29.49	40.28	36.38
Cooling	Baseline	0.31	0.40	0.26	0.61	0.46	0.41	0.56	0.50
	MPC	0.32	0.42	0.27	0.62	0.47	0.43	0.58	0.54
DHW	Baseline	32.38	32.35	32.39	32.34	32.36	32.36	32.37	32.36
	MPC	33.91	33.85	33.73	33.62	33.90	34.19	34.29	34.63
Costs [€/m²]									
Heating	Baseline	1.78	2.34	2.13	2.73	2.56	1.57	4.69	6.29
	MPC	1.74	2.30	2.10	2.68	2.51	1.50	4.50	5.97
Cooling	Baseline	0.02	0.02	0.02	0.05	0.03	0.03	0.06	0.13
	MPC	0.02	0.03	0.02	0.05	0.03	0.03	0.06	0.13
DHW	Baseline	1.84	1.92	1.93	2.38	2.31	1.83	3.41	6.45
	MPC	1.64	1.79	1.84	2.27	2.16	1.54	2.80	4.80

Table 6: Detailed yearly results per m^2 for the apartment block (AB).

Consumption [kWh/m²]		**2015**	**2016**	**2017**	**2018**	**2019**	**2020**	**2021**	**2022**
Heating	Baseline	20.09	26.11	23.88	25.71	23.29	18.64	26.81	23.31
	MPC	19.51	25.51	23.34	25.18	22.68	17.98	26.11	22.56
Cooling	Baseline	0.34	0.44	0.29	0.62	0.47	0.43	0.54	0.50
	MPC	0.36	0.46	0.30	0.63	0.49	0.45	0.56	0.55
DHW	Baseline	32.31	32.30	32.33	32.29	32.31	32.30	32.32	32.32
	MPC	33.81	33.77	33.63	33.54	33.82	34.10	34.22	34.58
Costs [€/m²]									
Heating	Baseline	1.13	1.57	1.38	1.82	1.67	0.99	3.20	4.16
	MPC	1.09	1.53	1.35	1.78	1.62	0.95	3.03	3.95
Cooling	Baseline	0.02	0.03	0.02	0.05	0.04	0.03	0.06	0.13
	MPC	0.02	0.03	0.02	0.05	0.04	0.03	0.06	0.12
DHW	Baseline	1.84	1.92	1.93	2.38	2.31	1.83	3.41	6.45
	MPC	1.64	1.79	1.84	2.26	2.16	1.54	2.80	4.80

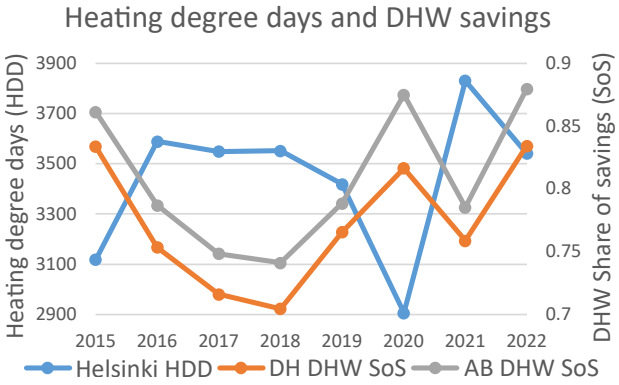

Figure 8: Heating degree days (HDD) in Helsinki [54] compared to the domestic hot water (DHW) share of savings (SoS).

of increasing it were analysed a bit further. Table 7 presents the relative increase in the achieved cost savings compared to the hourly 12-hour horizon cost-optimised MPC with respect to varying the optimisation interval and horizon. Increasing the optimisation horizon to 24 hours resulted in an 0.1–1.3 % and 0.2–4.6 % improvement in yearly savings for the DH and AB respectively, while increasing it further to 36 hours resulted in corresponding 0.1–1.7 % and 0.2–7.3 % improvements, depending on the simulated year. Even when using a horizon of 8760 hours, essentially optimising the full year at one go with perfect information, savings could only be improved by 0.2–3.0 % for the DH and by 0.9–9.8 % for the AB. Furthermore, using an optimisation horizon of 336 hours achieved essentially identical performance, indicating that the buildings either could not effectively store heat for longer than two weeks at most, or that the MPC rarely saw value in such long-term storage. Ultimately, considering that the most yearly savings for the DH and AB were able to achieve were 269 € and 3020 € in 2022 respectively, even the 3.0 % and 9.8 % increases are not overly significant. It is also worth noting, that in reality, uncertainty in future electricity prices and weather conditions would reduce these additional savings even further.

Table 7: Increases in yearly savings by optimisation interval and horizon relative to the hourly 12-hour horizon results presented in Table 4.

Detached house (DH)				
Interval [h]	**1**	**1**	**168**	**8736**
Horizon [h]	**24**	**36**	**336**	**8760**
2022 [%]	1.3	1.7	2.9	3.0
2021 [%]	0.8	1.2	2.1	2.1
2020 [%]	0.9	1.0	1.7	1.7
2019 [%]	0.4	0.4	0.5	0.5
2018 [%]	0.2	0.2	0.3	0.3
2017 [%]	0.1	0.1	0.2	0.2
2016 [%]	0.3	0.3	0.5	0.5
2015 [%]	0.6	0.6	0.8	0.8

Apartment block (AB)				
Interval [h]	**1**	**1**	**168**	**8736**
Horizon [h]	**24**	**36**	**336**	**8760**
2022 [%]	4.6	7.3	9.8	9.8
2021 [%]	3.6	5.9	8.4	8.4
2020 [%]	2.7	4.4	6.3	6.5
2019 [%]	0.6	0.7	1.5	1.5
2018 [%]	0.4	0.6	1.5	1.5
2017 [%]	0.2	0.2	0.9	0.9
2016 [%]	0.5	0.9	2.2	2.2
2015 [%]	0.7	1.1	2.6	2.6

The execution time for the results presented in Table 4 using a hourly 12-hour rolling horizon optimisation was around 23 minutes regardless of the year, with each solve taking less than a second on average. Similarly, for the four optimisation interval and horizon settings presented in Table 7 the execution times from left to right were roughly 24 min, 25 min, 25 s, and 50 s. In principle, Backbone could thus be used for real-time high-level economic MPC, although the presented simplified model lacks the necessary accuracy for actual control applications. Furthermore, while the speed of the full-year simulations could be improved by increasing the optimisation interval, solving optimal control only once a week or year is only possible with perfect information.

4 Discussion

The purpose of this paper was to demonstrate that the large-scale energy system model Backbone captures the essence of simple building-level MPC, facilitating studying the impacts of such MPC on the energy-system scale. Overall, the building-level MPC implemented using the Backbone energy system modelling framework behaved reasonably. Given hourly spot electricity price as the control signal, the MPC could be seen to exploit the available flexibility throughout the year in Figure 5, and consumption was observed shifting to hours of cheaper electricity in Figure 6.

In order to ensure the reliability of the desired behaviour, simulations were performed for years between 2015–2022, with the results presented in Table 4. The observed relative cost savings compared to the chosen baseline agree with existing literature [18, 55], again lending credence to the applicability of Backbone for capturing impacts of building-level MPC operations. Furthermore, the increasing volatility of electricity prices in the recent years resulted in increased cost savings from flexibility.

Compared to the DH, the AB achieved slightly better yearly cost savings, likely due to its larger DHW tank. The DHW tank was found to be responsible for roughly three quarters of the cost savings, despite accounting for only slightly more than half of the total yearly electricity demand as seen in Tables 5 and 6. The duration curves in Figure 7 illustrate that space heating and cooling flexibility was employed on relatively few hours when compared to the DHW tank due to not being economical. Calculating crude estimates for the flexibility of the interior air and DHW tank nodes by multiplying their thermal masses with their permitted temperature ranges suggests that the DHW should account for around 82 % of the available flexibility in both buildings, around the same order of magnitude as the achieved savings. While there is considerable thermal mass contained in the

structure nodes, their contribution to the space heating flexibility in this case seems minimal. However, this could potentially be improved by using e.g. underfloor heating, where heat can be more effectively stored in the structural mass of the building. Regardless, the above discussion is highly dependent on the assumed DHW tank sizing and technical properties, and more detailed models for the DHW tank and space heating are recommended in order to properly compare their flexibility.

Curiously, the space heating systems achieved larger shares of the generated savings for the DH than the AB, despite AB being more massive and energy efficient as evidenced by Tables 1, 2, 5, and 6. Similarly, Figure 8 indicates that the space heating systems achieved a larger share of the yearly savings during colder years with more heating demand, despite the increased heat losses from utilising the headroom in the indoor air temperature. It would seem that even though improved energy efficiency should allow for more efficient heat storage for the building interior, the accompanying reduction in the volume of shifted heating demand reduces the total generated savings compared to the DHW tank. However, this is again dependent on the technical properties of the modelled heating systems, and far-reaching conclusions should be left up to future research using more detailed building simulation models.

For practical MPC of buildings, the models used need to be able to run as often as there are meaningful updates to the input data. In the NordPool power exchange for example, the market is cleared once a day between 12:00–13:00 CET, determining the area prices for the next day. As a result, depending on the time of day, an MPC has anywhere between 12–36 hours of known future electricity prices. However, while the electricity prices might update only once every 24 hours, ambient conditions and occupancy in the building in question are in a constant flux, requiring more frequent evaluation of the predicted optimal control. The results using different optimisation intervals and horizons presented in Table 7 reflect this fact, with the results using a hourly interval simulating as close to real-time operation as possible with the used hourly time series data.

Looking at the results presented in Table 7, Backbone was able to achieve greater savings when the length of the optimisation horizon was increased. The magnitude of the improvements for the AB in particular were somewhat surprising in 2020–2022, although perfect information was used for simplicity. Typically, existing literature on building-level economic MPC tends to focus on horizons between 12–36 hours as determined by existing electricity market structures [56, 17], but for buildings with large DHW tanks and considerable thermal mass, it seems that such horizons might not be sufficient for capturing all the benefits of the inherent thermal storage capacity. That said, the additional savings achieved with horizons beyond 36 hours were practically negligible. Furthermore, in reality, as the length of the optimisation horizon increases, it becomes increasingly difficult to obtain good quality forecasts on future electricity prices, weather conditions, and occupant behaviour. Without good quality forecasts, the MPC risks making mistakes, reducing the amount of achieved savings. While employing either robust or stochastic optimisation could help mitigate the forecast-related risks, these methods also impact the expected savings. Lastly, increasing the length of the optimisation horizon inevitably also increases the computational time to solve each interval.

5 Conclusions

Overall, the performance of the building-level MPC implemented using the Backbone energy system optimisation framework was deemed reasonable. Given no incentive to utilise the flexibility in the space heating/cooling and water heating demands by providing the model with constant electricity prices, the model simply took minimum action necessary to maintain the required indoor air and DHW tank temperatures. On the other hand, minimising electricity costs against hourly spot prices resulted in utilising the thermal storage capacity inherent in the DHW tanks and building thermal mass to shift consumption to hours of cheap electricity. Furthermore, the resulting cost savings around 3.1–17.5 % agree with comparable values found in literature [55, 18], and could be seen to increase in recent years 2020–2022 at least

partly due to increased volatility in electricity prices. The impact of the used forecast horizon was deemed quite insignificant beyond the maximum day-ahead market horizon of 36 hours ahead of time.

The DHW tanks were found responsible of roughly three quarters of the cost savings, despite only accounting for slightly over half of the yearly electricity consumption. However, the simplified modelling approach used in this work could distort the results one way or the other, and more detailed models should be employed for a conclusive comparison. Furthermore, the flexibility of space heating could potentially be improved with different heat distribution systems or by temporarily falling to a set-back temperature if the situation allows. Regardless, DHW tanks seem capable of offering considerable flexibility with comparatively low practical complexity.

Integrating simplified building MPC into large-scale energy system modelling frameworks such as Backbone seems like a reliable approach for studying the impacts of widespread building-scale DSM on the operation of the overarching energy system. While this work focused on cost savings on the level of individual buildings for demonstration and validation purposes, the used approach has been designed primarily for energy-system scales required to quantify the system-level cost savings related to e.g. variable renewable energy integration and peak load reduction. However, further research is still required to compare building-level energy flexibility on an equal footing with grid-scale solutions in capacity expansion models.

A Abbreviations

AB	Apartment block
DH	Detached house
DHW	Domestic hot water
DSM	Demand-side management
G2WHP	Ground-to-water heat pump
HDD	Heating degree day
HVAC	Heating, ventilation, and air conditioning
MILP	Mixed-integer linear programming
MPC	Model-predictive control
RC	Resistance-capacitance
SPF	Seasonal performance factor

B Acknowledgements

This research was funded by the Academy of Finland project *Integration of building flexibility into future energy systems (FlexiB)* under grant agreement No 332421.

C CRediT authorship

Topi Rasku: conceptualisation, data curation, formal analysis, investigation, methodology, software, supervision, validation, visualisation, writing — original draft, writing — review and editing

Toni Lastusilta: conceptualisation, data curation, formal analysis, investigation, methodology, software, validation, visualisation, writing — original draft, writing — review and editing

Ala Hasan: conceptualisation, funding acquisition, project administration, resources, supervision, writing — review and editing

Rakesh Ramesh: conceptualisation, writing — original draft, writing — review and editing

Juha Kiviluoma: funding acquisition, project administration, resources, writing — review and editing

D Competing interests

The authors declare no conflict of interest. Furthermore, the funding agency had no role in the design of the study; in the collection, analyses, or interpretation of data; in the writing of the manuscript; or in the decision to publish the results.

E Data availability

The raw data, results, as well as the code used for processing the data for the simulations have been made available through Zenodo [36].

References

[1] Jochen Markard. The next phase of the energy transition and its implications for research and policy. *Nature Energy*, 3(8):628–633, 2018.

[2] Erdiwansyah, Mahidin, H. Husin, Nasaruddin, M. Zaki, and Muhibbuddin. A critical review of the integration of renewable energy sources with various technologies. *Protection and Control of Modern Power Systems*, 6(1), 2021.

[3] Peter D. Lund, Juuso Lindgren, Jani Mikkola, and Jyri Salpakari. Review of energy system flexibility measures to enable high levels of variable renewable electricity. *Renewable and Sustainable Energy Reviews*, 45:785–807, 2015.

[4] International Energy Agency (IEA). Buildings — Sectorial overview, 2022.

[5] International Energy Agency and United Nations Global Alliance for Buildings and Construction and Environment Programme. 2019 Global Status Report for Buildings and Construction: Towards a zero-emission, efficient and resilient buildings and construction sector. Technical report, International Energy Agency, 2019.

[6] International Energy Agency (IEA) and Tsinghua University. Building Energy Use in China — Transforming Construction and Influencing Consumption to 2050. Report, International Energy Agency (IEA), 2015.

[7] United States Environmental Protection Agency (EPA). Renewable Heating and Cooling — Renewable Space Heating, 2022-09-06 2022.

[8] Eurostat. Statistics Explained — Energy consumption in households, 2022-06 2022.

[9] Andreas Bloess, Wolf-Peter Schill, and Alexander Zerrahn. Power-to-heat for renewable energy integration: A review of technologies, modeling approaches, and flexibility potentials. *Applied Energy*, 212:1611–1626, 2018.

[10] Gabrielle Masy, Emeline Georges, Clara Verhelst, Vincent Lemort, and Philippe André. Smart grid energy flexible buildings through the use of heat pumps and building thermal mass as energy storage in the belgian context. *Science and Technology for the Built Environment*, 21(6):800–811, 2015.

[11] J. Le Dréau and P. Heiselberg. Energy flexibility of residential buildings using short term heat storage in the thermal mass. *Energy*, 111:991–1002, 2016.

[12] Thibault Q. Péan, Jaume Salom, and Ramon Costa-Castelló. Review of control strategies for improving the energy flexibility provided by heat pump systems in buildings. *Journal of Process Control*, 74:35–49, 2019.

[13] Yi Zong, Wenjing Su, Jiawei Wang, Jakub Krzysztof Rodek, Chuhao Jiang, Morten Herget Christensen, Shi You, You Zhou, and Shujun Mu. Model predictive control for smart buildings to provide the demand side flexibility in the multi-carrier energy context: current status, pros and cons, feasibility and barriers. In *10th International Conference on Applied Energy ICAE2018*, pages 3026–3031. Elsevier, 2019.

[14] Ján Drgoňa, Javier Arroyo, Iago Cupeiro Figueroa, David Blum, Krzysztof Arendt, Donghun Kim, Enric Perarnau Ollé, Juraj

Oravec, Michael Wetter, Draguna L. Vrabie, and Lieve Helsen. All you need to know about model predictive control for buildings. *Annual Reviews in Control*, 50:190–232, 2020.

[15] Anjukan Kathirgamanathan, Mattia De Rosa, Eleni Mangina, and Donal P. Finn. Data-driven predictive control for unlocking building energy flexibility: A review. *Renewable and Sustainable Energy Reviews*, 135, 2021.

[16] Jay H. Lee. Model predictive control: Review of the three decades of development. *International Journal of Control, Automation and Systems*, 9(3):415–424, 2011.

[17] Ye Yao and Divyanshu Kumar Shekhar. State of the art review on model predictive control (MPC) in Heating Ventilation and Air-conditioning (HVAC) field. *Building and Environment*, 200, 2021.

[18] Saman Taheri, Paniz Hosseini, and Ali Razban. Model predictive control of heating, ventilation, and air conditioning (HVAC) systems: A state-of-the-art review. *Journal of Building Engineering*, 60, 2022.

[19] Rasmus Halvgaard, Niels Kjølstad Poulsen, Henrik Madsen, and John Bagterp Jørgensen. Economic model predictive control for building climate control in a smart grid. In *2012 IEEE PES Innovative Smart Grid Technologies (ISGT)*, pages 1–6, 2012.

[20] Jingran Ma, Joe Qin, Timothy Salsbury, and Peng Xu. Demand reduction in building energy systems based on economic model predictive control. *Chemical Engineering Science*, 67(1):92–100, 2012. Dynamics, Control and Optimization of Energy Systems.

[21] Samuel R. West, John K. Ward, and Josh Wall. Trial results from a model predictive control and optimisation system for commercial building HVAC. *Energy and Buildings*, 72:271–279, 2014.

[22] Reino Ruusu, Sunliang Cao, Benjamin Manrique Delgado, and Ala Hasan. Direct quantification of multiple-source energy flexibility in a residential building using a new model predictive high-level controller. *Energy Conversion and Management*, 180:1109–1128, 2019.

[23] Behrang Vand, Reino Ruusu, Ala Hasan, and Benjamin Manrique Delgado. Optimal management of energy sharing in a community of buildings using a model predictive control. *Energy Conversion and Management*, 239, 2021.

[24] Bjarne Bach, Jesper Werling, Torben Ommen, Marie Münster, Juan M. Morales, and Brian Elmegaard. Integration of large-scale heat pumps in the district heating systems of Greater Copenhagen. *Energy*, 107:321–334, 2016.

[25] Jyri Salpakari, Jani Mikkola, and Peter D. Lund. Improved flexibility with large-scale variable renewable power in cities through optimal demand side management and power-to-heat conversion. *Energy Conversion and Management*, 126:649–661, 2016.

[26] Karsten Hedegaard and Olexandr Balyk. Energy system investment model incorporating heat pumps with thermal storage in buildings and buffer tanks. *Energy*, 63:356–365, 2013.

[27] Karsten Hedegaard and Marie Münster. Influence of individual heat pumps on wind power integration – energy system investments and operation. *Energy Conversion and Management*, 75:673–684, 2013.

[28] Samuel J.G. Cooper, Geoffrey P. Hammond, Marcelle C. McManus, and Danny Pudjianto. Detailed simulation of electrical demands due to nationwide adoption of heat pumps, taking account of renewable generation and mitigation. *IET Renewable Power Generation*, 10(3):380–387, 2016.

[29] Alessia Arteconi, Dieter Patteeuw, Kenneth Bruninx, Erik Delarue, William D'haeseleer, and

Lieve Helsen. Active demand response with electric heating systems: Impact of market penetration. *Applied Energy*, 177:636–648, 2016.

[30] Topi Rasku and Juha Kiviluoma. A Comparison of Widespread Flexible Residential Electric Heating and Energy Efficiency in a Future Nordic Power System. *Energies*, 12(1), 2018.

[31] David Huckebrink and Valentin Bertsch. Decarbonising the residential heating sector: A techno-economic assessment of selected technologies. *Energy*, 257, 2022.

[32] David Kröger, Jan Peper, and Christian Rehtanz. Electricity market modeling considering a high penetration of flexible heating systems and electric vehicles. *Applied Energy*, 331:120406, February 2023.

[33] Hans-Kristian Ringkjøb, Peter M. Haugan, and Ida Marie Solbrekke. A review of modelling tools for energy and electricity systems with large shares of variable renewables. *Renewable and Sustainable Energy Reviews*, 96:440–459, 2018.

[34] Xiwang Li and Jin Wen. Review of building energy modeling for control and operation. *Renewable and Sustainable Energy Reviews*, 37:517–537, 2014.

[35] Yanfei Li, Zheng O'Neill, Liang Zhang, Jianli Chen, Piljae Im, and Jason DeGraw. Grey-box modeling and application for building energy simulations - a critical review. *Renewable and Sustainable Energy Reviews*, 146, 2021.

[36] Topi Rasku. FlexiB Spine Toolbox workflow for Backbone model-predictive control data, 2023. Zenodo.

[37] EQUA Simulation AB and Aalto University. IDA Early Stage Building Optimization (ESBO), 2013. v1.13.

[38] Finnish Ministry of the Environment. D3 Rakennusten energiatehokkuus - Määräykset ja ohjeet 2012 (D3 Energy efficiency of buildings - Regulations and guidelines 2012), 30.3.2011 2011.

[39] Topi Rasku, Raimo Simson, and Juha Kiviluoma. Sensitivity of a simple lumped-capacitance building thermal modelling approach intended for building-stock-scale flexibility studies. Preprint. Zenodo, 2023.

[40] Adrian Chong, Yaonan Gu, and Hongyuan Jia. Calibrating building energy simulation models: A review of the basics to guide future work. *Energy and Buildings*, 253:111533, 2021.

[41] Finnish Ministry of the Environment. Ympäristöministeriön asetus uuden rakennuksen sisäilmastosta ja ilmanvaihdosta (Ministry of the Environment statute on the indoor climate and ventilation of new buildings), 2017.

[42] Jarek Kurnitski, Pekka Kalliomäki, Maarit Haakana, Jari Shemeikka, Ari Laitininen, Klobut Krzysztof, Mikko Saari, and Petri Kukkonen. Lämmitysjärjestelmät ja lämmin käyttövesi - laskentaopas (Heating systems and domestic hot water - calculation guide), 2011.

[43] Lari Eskola, Juha Jokisalo, and Kai Sirén. Lämpöpumppujen energialaskentaopas (Energy calculation guide for heat pumps), 2012.

[44] Topi Rasku. ArchetypeBuildingModel.jl, 2022. Version 2.1.3, GitHub and Zenodo.

[45] Fabian Hofmann, Johannes Hampp, Fabian Neumann, Tom Brown, and Jonas Hörsch. atlite: A lightweight python package for calculating renewable power potentials and time series. *Journal of Open Source Software*, 6(62), 2021.

[46] Hans Hersbach, Bill Bell, Paul Berrisford, Shoji Hirahara, András Horányi, Joaquín Muñoz-Sabater, Julien Nicolas, Carole Peubey, Raluca Radu, Dinand Schepers, Adrian Simmons, Cornel Soci, Saleh Abdalla, Xavier Abellan, Gianpaolo Balsamo, Peter Bechtold, Gionata Biavati, Jean Bidlot, Massimo Bonavita, Giovanna De Chiara, Per Dahlgren, Dick Dee, Michail Diamantakis, Rossana Dragani, Johannes Flemming, Richard Forbes, Manuel

Fuentes, Alan Geer, Leo Haimberger, Sean Healy, Robin J. Hogan, Elías Hólm, Marta Janisková, Sarah Keeley, Patrick Laloyaux, Philippe Lopez, Cristina Lupu, Gabor Radnoti, Patricia de Rosnay, Iryna Rozum, Freja Vamborg, Sebastien Villaume, and Jean-Noël Thépaut. The ERA5 global reanalysis. *Quarterly Journal of the Royal Meteorological Society*, 146(730):1999–2049, 2020.

[47] L. Gacitua, P. Gallegos, R. Henriquez-Auba, A. Lorca, M. Negrete-Pincetic, D. Olivares, A. Valenzuela, and G. Wenzel. A comprehensive review on expansion planning: Models and tools for energy policy analysis. *Renewable and Sustainable Energy Reviews*, 98:346–360, 2018.

[48] Anderson Rodrigo de Queiroz. Stochastic hydrothermal scheduling optimization: An overview. *Renewable and Sustainable Energy Reviews*, 62:382–395, 2016.

[49] Martin Håberg. Fundamentals and recent developments in stochastic unit commitment. *International Journal of Electrical Power & Energy Systems*, 109:38–48, 2019.

[50] Niina Helistö, Juha Kiviluoma, Jussi Ikäheimo, Topi Rasku, Erkka Rinne, Ciara O'Dwyer, Ran Li, and Damian Flynn. Backbone—an adaptable energy systems modelling framework. *Energies*, 12(17), 2019.

[51] ENTSO-E. Central collection and publication of electricity generation, transportation and consumption data and information for the pan-european market. Accessed 2023-01-10.

[52] Finnish Tax Administration. Tax rates on electricity and certain fuels. https://www.vero.fi/en/businesses-and-corporations/taxes-and-charges/excise-taxation/sahkovero/Tax-rates-on-electricity-and-certain-fuels/. Accessed 2023-01-05.

[53] John Forrest, Ted Ralphs, Haroldo Gambini Santos, Stefan Vigerske, John Forrest, Lou Hafer, Bjarni Kristjansson, jpfasano, EdwinStraver, Miles Lubin, Jan-Willem, rlougee, jpgoncal1, Samuel Brito, h-i gassmann, Cristina, Matthew Saltzman, tosttost, Bruno Pitrus, Fumiaki MATSUSHIMA, and to st. coin-or/Cbc, 2022. GitHub and Zenodo.

[54] Finnish Meteorological Institute (FMI). Heating degree days. Website. Accessed 2023-03-27. https://en.ilmatieteenlaitos.fi/heating-degree-days, 2023.

[55] Dongsu Kim, Jongman Lee, Sunglok Do, Pedro J. Mago, Kwang Ho Lee, and Heejin Cho. Energy Modeling and Model Predictive Control for HVAC in Buildings: A Review of Current Research Trends. *Energies*, 15(19), 2022.

[56] Abdul Afram and Farrokh Janabi-Sharifi. Theory and applications of HVAC control systems – A review of model predictive control (MPC). *Building and Environment*, 72:343–355, 2014.